Subharmonic All-Optical Clock Recovery of up to 320 Gb/s Signal Using a Quantum Dash Fabry–Pérot Mode-Locked Laser

Josué Parra-Cetina, Jun Luo, Nicola Calabretta, Sylwester Latkowski, Harmen J. S. Dorren, and Pascal Landais

In this study, we provide an experimental assessment of a quantum dash Fabry–Pérot mode-locked laser for all-optical clock recovery using data streams at 40, 80, 160, and 320 Gb/s. The data streams at 80, 160, and 320 Gb/s are phase coherent signals featuring no spectral component at 40 GHz. The 40 GHz recovered optical clock signal is characterized in terms of phase noise, timing jitter, dynamic power range, and wavelength dependence for the different data rates. Our experiments demonstrate a recovered optical clock signal from a 320 Gb/s data stream with a timing jitter of 94 fs and wavelength detuned by 23 nm. In addition, the performance of the optical time division multiplexing receiver at 80 and 160 Gb/s data signals employing the recovered clock as a demultiplexing control signal and as a clock for the bit-error-rate tester (BERT) is evaluated by bit error rate measurements on the demultiplexed data signals.

Bit error rate (BER) measurement, clock recovery, mode-locked laser, optical time division multiplexing (OTDM), quantum dash, time-demultiplexing, timing jitter.

I. Introduction

ALL-OPTICAL clock recovery (OCR) and optical demultiplexing (OD) are key functionalities in the optical receiver frontend for high-speed optical time division multiplexing (OTDM) networks. Current clock recovery (CR) schemes are based on optoelectronic phase-locked loops [1]–[3]. However, the use of a feedback loop increases the complexity, and the cost of the system. On the other hand, CR operations have been investigated by using mode-locked semiconductor laser diodes (MLLD) [4]–[7]. Such devices have attracted significant attention because of their stable operation, cost effectiveness, low energy consumption, and small size. Among the different approaches for CR with MLLDs, those based on quantum dot/dash (QDot/QDash) lasers have achieved good performance in terms of frequency stability and low timing jitter [9] because of their narrow beat-tone linewidth and small associated phase noise [9]–[11]. Furthermore, QDash-MLLD have demonstrated the feasibility to synchronize their free running frequencies lying at ∼40 GHz with high bit rates at 40 Gb/s and beyond by direct [6], [9] or subharmonic frequencies [8], [12], as well as being able to handle both non-return-to-zero (NRZ) and return-to-zero (RZ) modulation using both conventional and complex formats [11]. Moreover, the fast locking time of the QDash-MLLD allows the possibility to exploit the OCR for burst mode operation [13]. Although an OCR based on a QDash-MLLD followed by a high-speed photodetector and an electro-optical modulator as time demultiplexing has been recently demonstrated for optical signals up to 160 Gb/s [14], QDash-MLLD-based OCR operation using high-speed return-to-zero on-off keying (RZ-OOK) featuring no component at 40 GHz has never been demonstrated. This is a serious issue, as any 40 GHz component strongly contributes to the synchronization of 40 GHz free running frequency of the MLLD.

In this study, we experimentally assess the operation and the performance of a QDash-MLLD-based all-optical subharmonic CR for up to 320 Gb/s coherent RZ-OOK signals. The quality of the 40 GHz clock signal is evaluated by phase noise, timing jitter, power dynamic range, wavelength operation, and pattern length measurements.

This paper is organized as follows. In section II, we present the intrinsic performances of the QDash-MLLD. Subsequently, in Section III an analysis of the recovered clock is performed when synchronized to a baseline 40 Gb/s data rate. The performance assessment of the CR for data rate up to 320 Gb/s is presented in section IV. In Section V, the operation of the OTDM receiver at 80 and 160 Gb/s employing the recovered clock for controlling an optoelectronic time demultiplexing system and for clocking the BERT is investigated. Section VI concludes the paper.

II. Passively Mode-Locked Quantum Dash Laser

The device under investigation is a 1-mm long, dc-biased, multimode QDash Fabry–Pérot mode locked laser diode [15], in a butterfly package fabricated by Archay Ltd. The laser is a single-section device, without phase or saturable absorption sections. Its threshold current is measured at 18 mA and an average power of 4.7 mW is collected by a pigtail patchcord when operating at 350 mA and temperature controlled at 25 °C. Within the

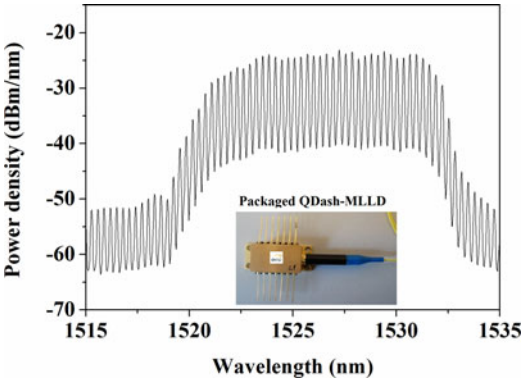

Fig. 1. Optical spectrum of the QDash-MLLD biased at 120 mA, inset: photograph of the packaged QDash-MLLD.

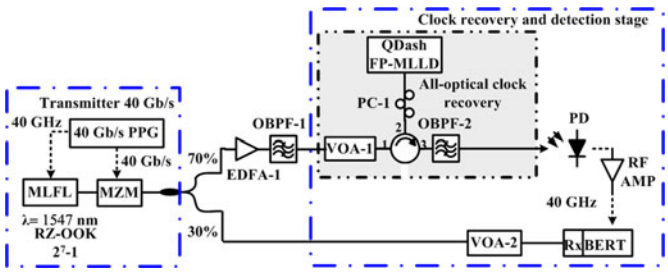

Fig. 2. Experimental setup of the all-optical clock recovery from 40 Gb/s RZ-OOK.

3 dB spectral bandwidth, the QDash-MLLD exhibits 40 modes spanning from 1520 to 1532 nm with an intermodal separation of 0.31 nm, corresponding to a 39.77 GHz free spectral range (FSR). Fig. 1 shows the optical spectrum of the QDash-MLLD, the inset shows a photograph of the packaged laser under study. In addition, the linewidth of the longitudinal modes varies from 10 to 45 MHz [16]. Despite being dc-biased, the laser exhibits passive mode-locking behavior, featuring a periodic variation of its output emission. Mode-locking in this type of laser is attributed to the nonlinearities in the semiconductor active region, mainly sustained by four wave mixing processes [11], [15]–[17]. The frequency of the RF beat-tone is determined by the laser's FSR, and features a FWHM of 25 kHz at free running conditions. The pulses generated by the laser have duration of 2.2 ps, and a time-bandwidth product of around 0.84 [16].

III. 40 Gb/s Clock Recovery Setup

The first part of the experiment is to investigate the clock-recovery functionality based on a QDash-MLLD operating under injection of an optical data stream RZ-OOK at 40 Gb/s and controlled at room temperature ∼25 °C. Fig. 2 illustrates the CR experimental setup. It consists of two major blocks: an OTDM RZ-OOK transmitter and the CR system based on the QDash-MLLD. In the OTDM RZ-OOK transmitter, a 40 GHz short pulse, featuring 1.3 ps pulse width, from a mode-locked fiber laser (MLFL) is modulated by a 40 Gb/s 2^7–1 or 2^{31}–1 long pseudorandom binary sequence (PRBS), to produce the 40 Gb/s RZ-OOK signal. The 2^{31}–1 long PRBS will be only used when analyzing and comparing the clock recovery dependence to pattern length in Section B. Fig. 3(a) shows its optical spectrum recorded by an optical spectrum analyzer with a resolution of 0.06 nm and the eye-diagram of this optical data signal which is characterized by a 18.95 dB extinction ratio. The center wavelength of the 40 Gb/s is located at 1547 nm, and its spectral width is limited to 1.5 nm by an optical bandpass filter (not depicted in Fig. 2). The signal is split with 30% of the power sent to the detection stage for BER measurements, while the remaining 70% is sent to the all-optical CR block. First, the optical signal is amplified with an Erbium-doped fiber amplifier (EDFA-1). An optical band-pass filter (OBPF-1) centered at 1547 nm and bandwidth of 5 nm suppresses a part of the amplified spontaneous emission from EDFA-1. This optical data stream signal is injected into the QDash-MLLD via an optical circulator. A polarization controller (PC-1) is required to optimize the state of polarization of the injected signal. The optical power of the injected signal is in the range of –3 to +4 dBm controlled by a variable optical attenuator (VOA-1). The QDash-MLLD is dc-biased at 120 mA and temperature stabilized at 25 °C. The optical spectrum at the output of the locked QDash-MLLD is shown in Fig. 3(b). The figure shows the MLLD's emission centered at 1527 nm and the spectrum at 1547 nm due to the reflection of the injected optical signal at the input facet of the MLLD. The recovered optical clock is filtered out through OBPF-2 centered at 1530 and 5 nm bandwidth which is utilized to spectrally isolate the recovered clock at the QDash-MLLD output from the reflected injected data stream. Fig. 3(c) shows this optical spectrum of the recovered clock. Inset shows the time trace of the recovered clock retrieved by an optical sampling oscilloscope.

The optical clock is then converted to the electrical domain by using a 50 GHz photodetector (PD) and a 40-GHz RF amplifier (RF-AMP) for triggering a bit error (BER) tester or to assess the recovered clock in the RF domain with an electrical spectrum analyzer (ESA). Fig. 3(d) shows the RF spectrum of the QDash–MLLD in free running (black) and the one synchronized to the 40 Gb/s RZ-OOK signal (red). The reduction in the RF linewidth in the locking state is clearly visible, as compared to free running. The RF linewidth of the synchronized clock exhibits a value of $<$1 kHz, when measured with a span of 1 kHz and resolution bandwidth of 20 Hz. This is in agreement with previous studies of mode locking with this kind of devices [18], [19]. Fig. 3(e) shows the single sideband phase noise spectrum density (SSB-PSD) of the recovered 40 GHz clock, retrieved from the ESA, as well as the accumulated timing jitter. The phase noise trace of the original 40 GHz clock from transmitter is also shown as a reference in Fig. 3(e). From this figure, it is possible to observe that reference clock is noisier than recovered clock at low frequencies which increases its timing jitter. After a frequency of 200 kHz, the recovered clock presents more noise and consequently there is an increase on its associated timing jitter.

In order to evaluate the timing jitter σ_J and to confirm the measurement retrieved from the ESA, we have [20]:

$$\sigma_J = \frac{1}{2\pi f_R}\sqrt{\int_{f\ \min}^{f\ \max} L(f)\,\mathrm{d}f} \qquad (1)$$

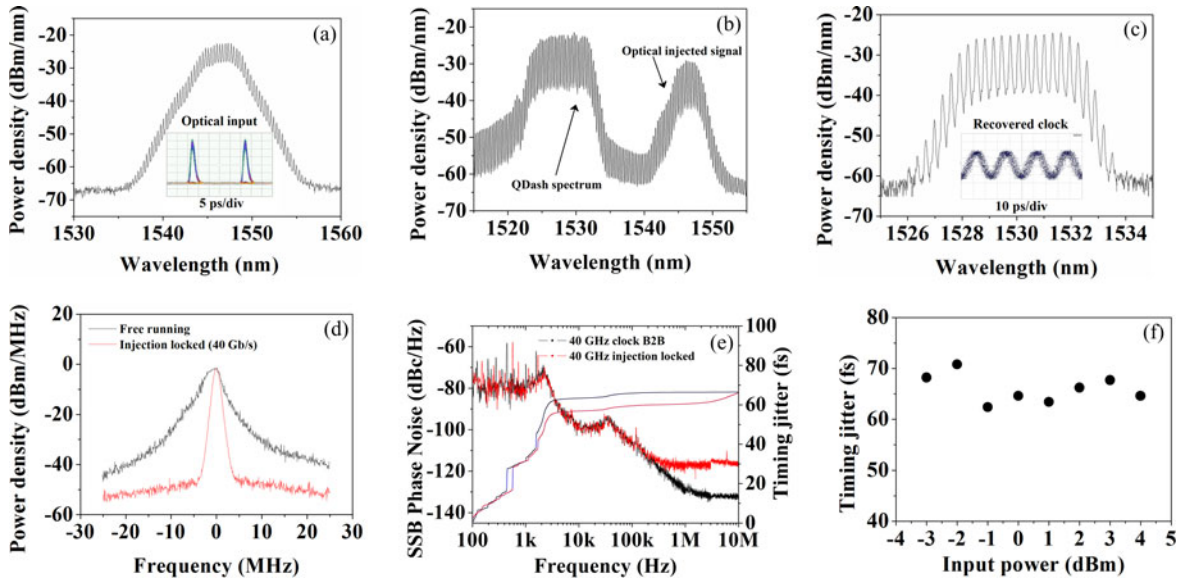

Fig. 3. Optical spectra: (a) 40 Gb/s RZ-OOK optical input, inset signal. Inset: time trace, horizontal, and vertical scales are 5 ps/div and 10 mV/div, respectively., (b) QDash-MLLD output before filtering. (c) Recovered clock. Inset: time trace, horizontal, and vertical scales are 10 ps/div and 100 mV/div, respectively. (d) Comparison of the RF spectra at QDash-MLLD output, free running and injection locked. ESA set at resolution of 1 MHz and span of 50 MHz. (e) Comparison of the single side band phase noise of back-to-back and recovered clock; (f) Timing jitter versus input power of recovered clock from QDash-MLLD.

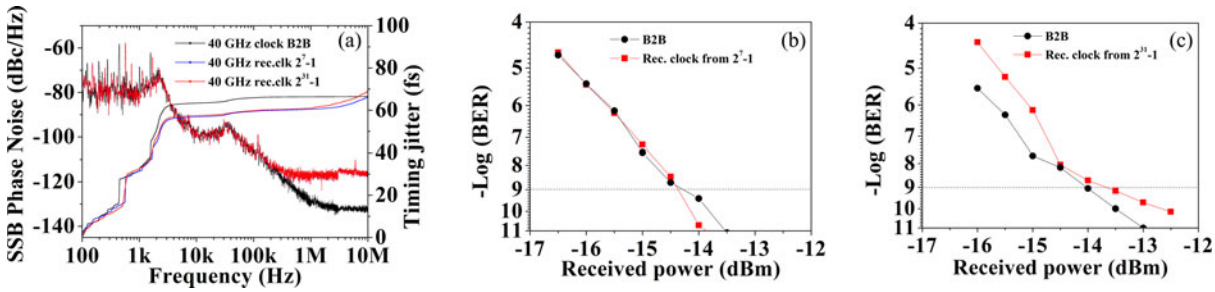

Fig. 4. (a) Comparison of single side band phase noise of back to back and recovered clock under injection of RZ-OOK signals at different pattern length. (b) BER results for an input with a pattern length 2^7 –1; black dots, B2B; red squares, recovered clock. (c) BER results for an input with pattern length 2^{31} –1; black dots B2B; red squares, recovered clock.

where $L(f)$ is the phase-noise spectral density (referred in the rest of the text as single sideband phase noise spectral density (SSB-PSD)), f_R is the repetition-rate, and $f$min and $f$max are boundaries of the frequency range. For the values of timing jitter reported in this paper, the integration boundary is from 100 Hz to 10 MHz. The recovered 40 GHz clock has a timing jitter of 66 fs.

A. Dynamic Power Locking Range

The determination of the dynamic power locking range is achieved by varying the optical power injected into the QDash-MLLD while preserving the same driving bias current to the QDash-MLLD, and no optimization of the state of polarization of the input signal is sought. The optical power is varied from –3 dBm to +4 dBm at the input of the packaged QDash-MLLD. The initial state of the QDash-MLLD is in free-running and then a given power is injected. The phase noise trace of the RF signal of the recovered clock is analyzed. Fig. 3(f) shows the timing jitter dependence of the QDash-MLLD as a function of the injection optical power. The timing jitter of the synchronized QDash-MLLD presents almost a flat behavior. This indicates that once the QDash-MLLD is locked, it is stable and the phase noise and the associated timing jitter are approximately constant with an average value of 65 fs.

B. Clock Recovery Pattern Length Dependence

The additional investigation of the CR is performed by analyzing the BER measurements on the incoming data signal synchronized by the recovered clock for 2^7–1 long and 2^{31}–1 long patterns. Fig. 4(a) shows the single sideband phase noise spectrum density (SSB-PSD) of the recovered 40 GHz for the two pattern lengths. The recovered clock has a timing jitter of 66 fs and 69.1 fs for 2^7–1 and 2^{31}–1 long patterns, respectively. Fig. 4(b) and (c), depicts a comparison between the BER curves measured with a back-to-back (B2B) electrical clock from the transmitter, and with the clock synchronized to the 40 Gb/s (2^7–1) long data sequence (see 4(b)) and to the (2^{31}–1) long data sequence (see 4(c)). It is possible to determine that there is no penalty for CR for an input signal with 2^7–1 long pattern, while a penalty of 0.5 dB exists for the recovered clock for an input

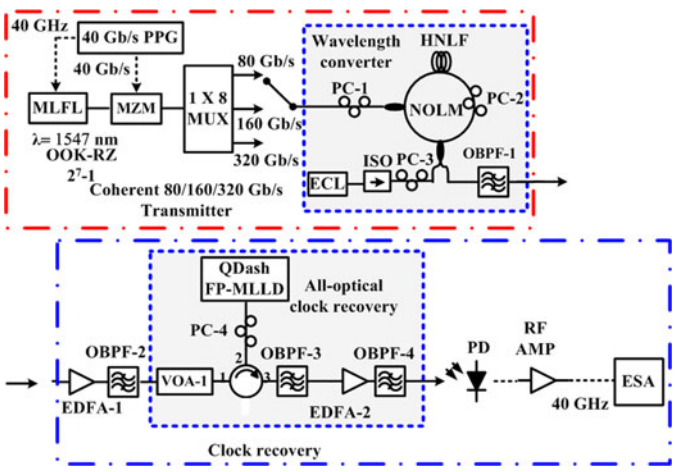

Fig. 5. All-optical clock recovery experimental setup for high speed RZ-OOK.

signal with 2^{31}–1 long pattern. The operational conditions of the QDash-MLLD in terms of temperature are similar for both data pattern lengths, but not in terms of bias current and optical injected power, being 100 mA and –1 dBm for 2^7–1 long pattern and 150 mA and 1 dBm for 2^{31}–1 long pattern.

IV. Subharmonic Clock Recovery

The subharmonic CR experimental setup is shown in Fig. 5. It consists of two major blocks: an OTDM RZ-OOK transmitter in the red box and the CR system based on the QDash-MLLD in the blue box. In the OTDM RZ-OOK transmitter, the 80, 160, and 320 Gb/s OTDM RZ-OOK signals are generated by optically time multiplexing a 40 Gb/s data stream via a fiber-based interleaver. The resulting 80, 160, and 320 Gb/s RZ-OOK have a data pattern of 2^7–1 long RZ-OOK PRBS due to the limit of the time interleaver, and have a central wavelength of 1547 nm. It is possible to observe in Fig. 6 that the optical spectra of the signal at 80, 160, and 320 Gb/s contain a remaining 40 GHz spectral component originated by the MLFL. In order to obtain a stable and phase coherent RZ-OOK signal, the original OTDM signal is wavelength converted. As it is shown in Fig. 5, the 80, 160, or 320 Gb/s OTDM are fed into a nonlinear optical loop mirror (NOLM)-based wavelength converter (WC) as the control signal, while a coherent CW light ($\lambda_s = 1558$ or 1559 nm) is used as the probe.

The principle of operation of the NOLM-based wavelength converter is reported in [21] and [22]. At the output of the NOLM, the data information of the 80, 160 or 320 Gb/s RZ-OOK sequence are replicated to the coherent CW probe light. At its output, a 6 nm optical band-pass filter with the center wavelength located at the coherent CW light is used to select out the phase coherent 80, 160, or 320 Gb/s RZ-OOK signal. The coherent data signal is then launched into the all-optical CR setup based on the QDash-MLLD. The extracted clock is photodetected and amplified by an RF amplifier. The retrieved electrical clock is analyzed through an ESA.

Fig. 6 represents the optical spectra of wavelength conversion, in red, and of the phase coherent RZ-OOK signals after filtering

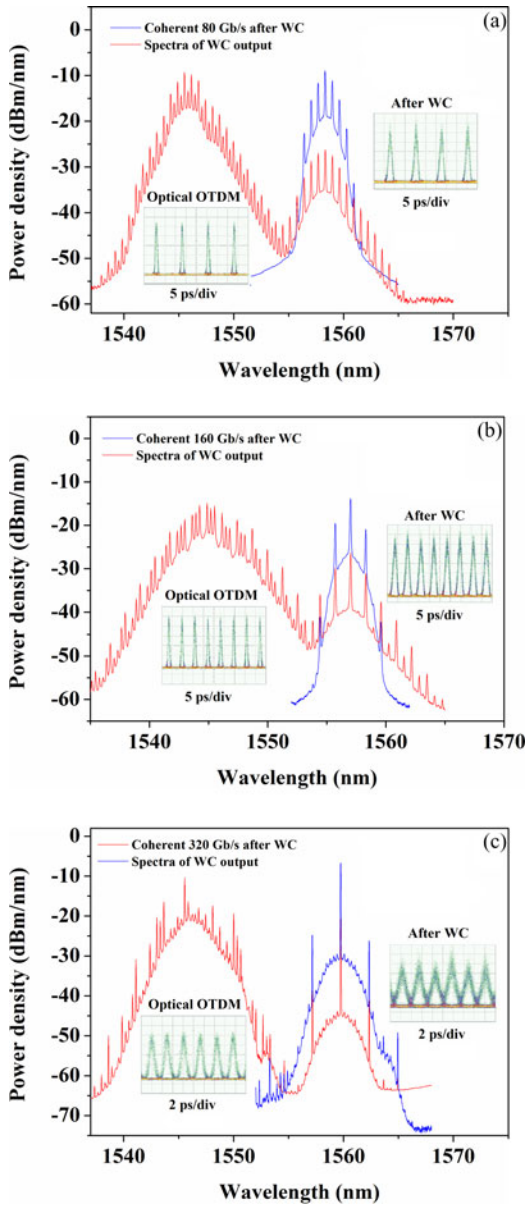

Fig. 6. Optical spectra at the output of WC: (a) for input at 80 Gb/s, with RBW: 0.06 nm. Inset: time traces of the corresponding signals, x-scale 5 ps/div.; (b) for input at 160 Gb/s, with RBW: 0.06 nm. Inset: time traces of the corresponding signals, x-scale 5 ps/div.; (c) for input at 320 Gb/s, with RBW: 0.06 nm. Inset: time traces of the corresponding signals, x-scale 2 ps/div.

by OBPF-1 and 13 dB of amplification in blue, for a bit-rate of 80 Gb/s (a), 160 Gb/s (b) and 320 Gb/s (c), respectively. Before the filtering stage (OBPF-1), the WC spectra are characterized by a main peak at 1547 nm (control signal) and a secondary peak at 1558 or 1559 nm (the former in the case of input signals at 80 Gb/s and 160 Gb/s, the latter in the case of 320 Gb/s) due to the probe signal. After filtering, it can be clearly observed that the coherent signals produced at 80, 160, and 320 Gb/s are free of the 40 GHz component and phase jump inherent to OTDM [23]. The separation between optical modes is measured as 0.66, 1.32, and 2.64 nm, resulting from the bit-rate of the transmitter, at 80, 160, and 320 Gb/s, respectively. The insets present the eye diagrams of the optical input data signals before

WC and after WC at 80, 160, and 320 Gb/s, respectively. The pulses are separated by 12.5 ps (a), by 6.25 ps (b) and by 3.125 ps (c), respectively.

Such optical data signals are fed into the all-optical recovery system. The 40 GHz subharmonic optical CR is achieved by injection locking the QDash-MLLD. The QDash-MLLD is operated with low bias current of 86 mA, controlled at room temperature at 25 °C and polarization. The polarization dependence can be solved by cascading a bulk and a quantum dash mode-locked laser [24]. The injection power is within the range of 4 and 5 dBm in the case of incoming signals at 80 and 160 Gb/s, respectively. For 320 Gb/s, another QDash-MLLD with similar characteristics as the one employed for 80 and 160 Gb/s was employed. However, it was not possible to demonstrate the synchronization of the QDash-MLLD at room temperature, due to the high bit rate that interacted in the laser cavity. In order to achieve the synchronization of the QDash-MLLD and therefore the CR at such a bit rate, its operational conditions such as the bias current and temperature were changed to 117 mA, 21.7 °C, respectively. Furthermore, the optical injection power was increased to 7 dBm. Fig. 7 represents the optical output of the QDash-MLLD under injection before filtering from OBPF-3, in red, and of the recovered clock (after filtering) in blue, at bit rates of 80, 160, and 320 Gb/s, respectively. In all these figures, it is noted that the injected and recovered clock signals are detuned by more than 23 nm.

The synchronized signal centered at 1532 nm features a free-spectral range of 0.33 nm, corresponding to a rate of 40 GHz. Even though the injected signals are at 80, 160, or 320 Gb/s, the synchronized signal is invariably set at 40 GHz. The QDash-MLLD is therefore able to synchronize to an incoming data signal at a multiple of its internal free-running frequency.

A. *Characterization of the Recovered Clock Signal*

This section is dedicated to the analysis of the response of the QDash-MLLD under optical injection of 80, 160, and 320 Gb/s data sequence. Fig. 8(a) reports the RF spectra due to the beating of the lasing modes at the photodiode. The figure has been offset by 40 GHz. The free-running spectral density of the beating presented in black, features a Lorentzian distribution with a 25 kHz linewidth, which is largely narrower than that of any of the optical longitudinal modes as already shown in Fig. 1. Since the laser beating linewidth results from the phase noise of the optical modes, the phase noise of each mode must be correlated. An intracavity FWM has been proposed to explain the mode correlation [25]. The synchronized RF beating spectra at 80, 160, and 320 Gb/s (green, blue, and red traces, respectively) are shown in Fig. 8(a), retrieved with a span of 50 MHz and resolution bandwidth of 1 MHz. For the three traces, when measured at a span of 1 kHz and resolution bandwidth of 20 Hz, they exhibit a RF linewidth of $<$1 kHz. This compression of the RF linewidth and change in distribution confirm the synchronization of the QDash-MLLD to the optical injected signals. The difference between the RF spectra when synchronized to 80, to 160, and to 320 Gb/s is attributed to different operational conditions of the QDash-MLLD (as mentioned previously) for

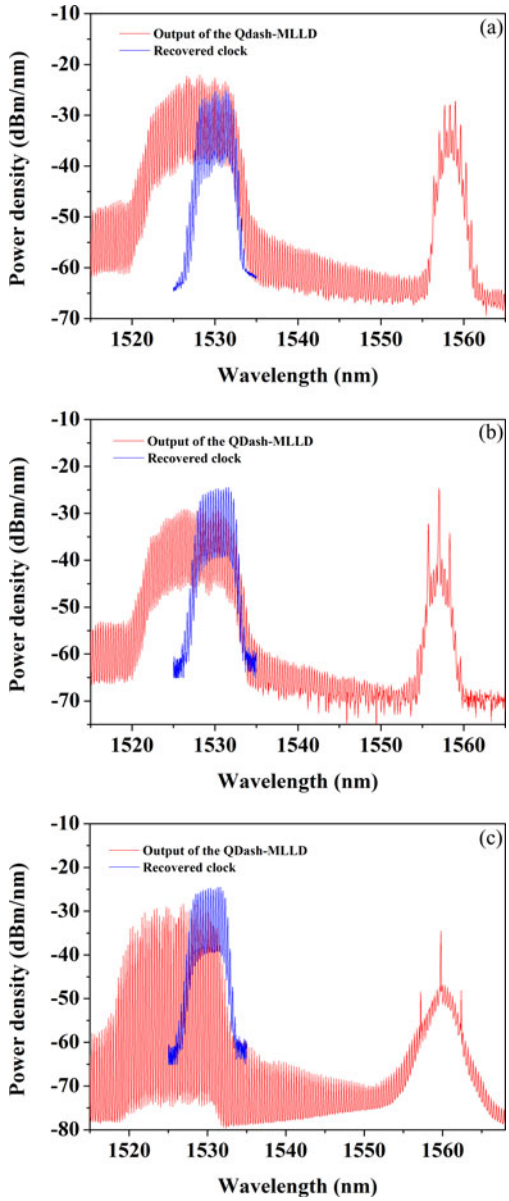

Fig. 7. Optical spectra at the output of the QDash-MLLD for input data rates of: (a) 80 Gb/s, (b) 160 Gb/s, and (c) 320 Gb/s.

which the synchronization is achieved, [see Fig. 8(a)]. Fig. 8(b) exhibits the SSB-PSD of the back-to-back 40 GHz clock signal, i.e. the electrical clock signal provided by transmitter. The timing jitter accumulated from 100 Hz to10 MHz is 50 fs. The 40 GHz recovered clock signal under injection of the 80 Gb/s coherent wavelength converted signal has a timing jitter of 62 fs. In the same condition, but under injection of 160 Gb/s, the timing jitter is 92 fs. The SSB-PSD of the recovered clock under injection of 320 Gb/s exhibits a higher value, resulting in more accumulated timing jitter than for the other injected data rates, featuring 94 fs.

B. *Dynamic Power Locking Range*

The assessment of the dynamic power locking range for optical injection of 80, 160, and 320 Gb/s data sequence is achieved

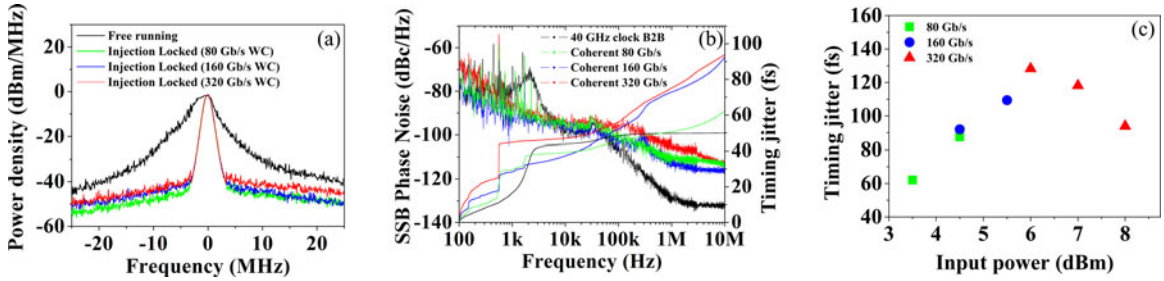

Fig. 8. (a) Comparison of the RF spectra at QDash output, free running, and locking conditions with a frequency span of 50 MHz and the resolution bandwidth of 1 MHz. (b) Comparison of single side band phase noise of back to back with recovered clock under injection of coherent 80, 160, and 320 Gb/s RZ-OOK; (c) Timing jitter versus input power of recovered clock from QDash-MLLD under injection of coherent 80, 160, and 320 Gb/s RZ-OOK.

by varying the optical power injected into the QDash-MLLD while preserving the same driving bias current to the QDash-MLLD, and no optimization of the state of polarization of the input signal is sought. The optical input power is controlled to vary from 3.5 to 4.5 dBm for an optical input data rate at 80 Gb/s, from 4.5 to 5.5 dBm at 160 Gb/s and from 6 to 8 dBm at 320 Gb/s. The RF signal of the recovered clock is analyzed by retrieving the phase noise trace and calculating the accumulated timing jitter.

Fig. 8(c) shows the timing jitter dependence of the recovered clock from QDash-MLLD as a function of the optical input power at data rates of 80, 160, and 320 Gb/s. From Fig. 8(c), two important results are found. First, the dynamic range at 80 and 160 Gb/s is 1 dB and both present an increment in the timing jitter as the optical input power increases. These traces are labeled with green squares for 80 Gb/s and blue circles for 160 Gb/s, averaging timing jitter values of 75 and 100 fs, respectively. This increase in the timing jitter with the increase in optical power injected is due to the added noise from the EDFA-1 and the induced wavelength shift between the QDash-MLLD and the input signals at such data rates. The shift of the QDash-MLLD longitudinal spectrum is a consequence of variations in the gain and refractive index of the cavity under high power injection. The timing jitter of the synchronized QDash-MLLD at 320 Gb/s data sequence presents a decreasing trend with the increase of input power, labeled in red triangles. This indicates that the interaction among the modes in the QDash-MLLD with the wavelength of the input signal at this data rate is better detuned with the increment in power, giving rise to an enhancement of the phase correlation of the QDash-MLLD, averaging 110 fs. The second result derived from Fig. 8(c), one that complements the results provided in section A, is that in order to achieve the synchronization of the QDash-MLLD at higher bit rates it is necessary to increase the power injected into the QDash-MLLD, leading to an increase in the phase noise and associated timing jitter but decreasing the dynamic power locking range when compared to the results derived from a base-line synchronization.

V. OTDM Receiver Based on the QDash Clock Recovery

As demonstrated in previous section, the recovered clock from the high speed data rates used in this study presents a low

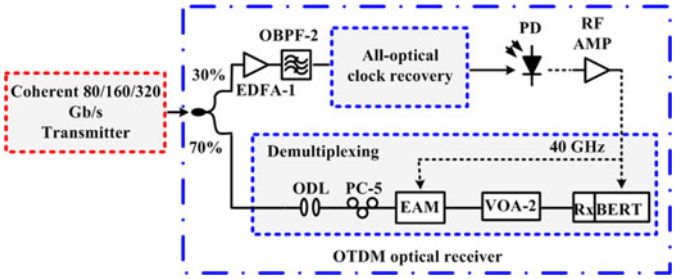

Fig. 9. OTDM receiver experimental setup for demultiplexing of high-speed RZ-OOK.

timing jitter. This feature allows the use of the recovered clock to demultiplex the incoming signal into tributaries at 40 Gb/s. From Fig. 9, the synchronized 40 GHz optical pulses, after being photodetected and amplified are fed into an electroabsorption modulator (EAM) optical demultiplexer to select each of the two or four 40 Gb/s tributaries of the 80 and 160 Gb/s signals, respectively. This selection of channels is performed through the optical delay line (ODL).

The obtained 40 Gb/s channels are then detected and tested by a bit error rate (BER) tester, which is also triggered by using the recovered 40 GHz clock. It is worth mentioning, that it is not possible to demultiplex the OTDM 320 Gb/s signal with this scheme, since, beyond 160 Gb/s the switching window of OTDM based on fast electro-optical-modulators (EOM) is too large to resolve the high-speed modulated pulses. This leads to a larger crosstalk as the data rate increases, and thus to a larger power penalty.

The BER results are given in Fig. 10 to quantify the performance of the 80 to 40 Gb/s and 160 to 40 Gb/s demultiplexers. In Fig. 10(a), the 80 Gb/s back-to-back (B2B) BER curves labeled by a black dot and the BER curves of the 80 Gb/s after WC curves demultiplexed by using the original electrical clock, labeled with red squares, are reported as references. The 80 Gb/s BER curves after wavelength conversion and demultiplexing by using the recovered optical clock are labeled with a blue star. It can be seen from these curves that the optical synchronized signal can be used as a 40 GHz optical clock for demultiplexing of optical signals achieving error free for an optical injection of at least –12 dBm. A power penalty of 1.5 dB is measured when compared with the B2B. The source of this penalty is mostly due to the pulse broadening of the input signals after the

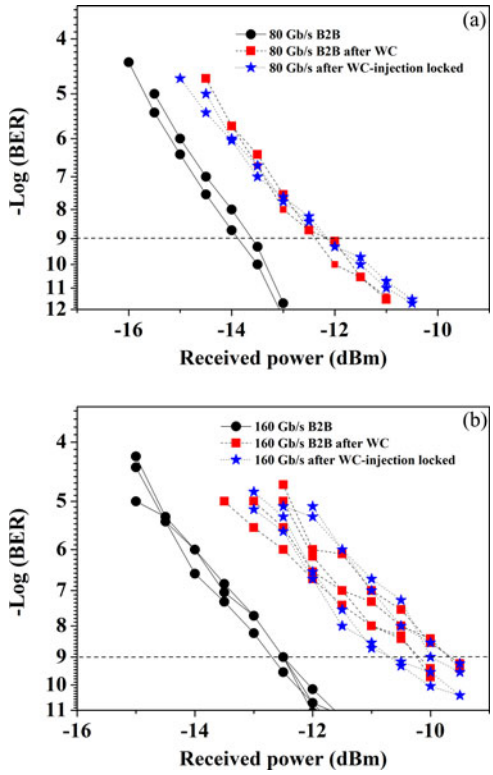

Fig. 10. (a) BER results for an input at 80 Gb/s; black dots, B2B; red squares, B2B after WC; blue stars, after WC and using recovered clock (b) BER results for an input at 160 Gb/s; black dots, B2B; red squares, B2B after WC; blue stars, after WC and using recovered clock.

wavelength conversion scheme at this bit-rate. Similar experiments have been carried out at 160 Gb/s [see Fig. 10(b)]. In the case of 160 Gb/s, four 40 Gb/s tributaries are demultiplexed. It can be observed that when the power dependence of the BER of the original B2B 160 Gb/s OTDM signal is compared with that of the phase coherent 160 Gb/s RZ-OOK, a 1.5 dB penalty is observed. It can be concluded that the WC is the main source of power penalty. This is due to the data pulse broadening and extra amplitude noise introduced during the wavelength conversion. In addition, by comparing between the BER traces of the phase coherent 160 Gb/s RZ-OOK, while using the original clock and recovered clock, respectively, it is found that there is negligible penalty between the two cases, which indicates that the recovered clock has a comparable quality with the original clock.

VI. Conclusion

We have experimentally characterized the operation of a quantum dash Fabry–Pérot mode locked laser in an all-optical CR scheme for data streams up to 320 Gb/s. Phase noise and timing jitter, dynamic power range, and wavelength dependence of the 40 GHz recovered optical clock signal were investigated for different data rates. Experimental results show the recovered optical clock signal from a 320 Gb/s data stream with a timing jitter of 94 fs and wavelength detuned by 23 nm.

We have also assessed the performance of the OTDM receiver at 80 and 160 Gb/s data signals employing the recovered clock as a demultiplexing control signal and as clock for the BERT. By using the synchronized optical clock to demultiplex the 80 and 160 Gb/s, power penalties of 1 and 1.5 dB were measured, respectively.

The main advantages of the all-optical CR based on the QDash-MLLD are compactness, simple operation, stability, low cost, and low power consumption. Indeed, no high speed opto-electronic circuitries are needed since the QDash-MLLD is able to generate a 40 GHz pulse train by simply applying dc-bias. It is clear from the results obtained in these experiments that the QDash-MLLD is a reliable and cost-effective solution to all-optical signal processing.

References

[1] L. K. Oxenlowe, F. Gomez-Agis, C. Ware, S. Kurimura, H. C. H. Mulvad, M. Galili, H. Nakajima, J. Ichikawa, D. Erasme, A. T. Clausen, and P. Jeppesen, "640-Gbit/s data transmission and clock recovery using an ultrafast periodically poled lithium niobate device," *J. Lightw. Technol.*, vol. 27, pp. 205–213, Feb. 2009.

[2] H. C. H. Mulvad, E. Tangdiongga, H. de Waardt, and H. J. S. Dorren, "40 GHz clock recovery from 640 Gbit/s OTDM signal using SOA-based phase comparator," *Electron. Lett.*, vol. 44, pp. 146–147, Jan. 2008.

[3] N. Jia, T. Li, K. Zhong, J. Sun, M. Wang, and J. Li, "Simultaneous clock enhancing and demultiplexing for 160-Gb/s OTDM signal using two bidirectionally operated electroabsorption modulators," *IEEE Photon. Technol. Lett.*, vol. 23, pp. 1615–1617, Nov. 2011.

[4] T. Ohno, K. Sato, T. Shimizu, T. Furuta, and H. Ito, "Recovery of 40 GHz optical clock from 160 Gbit/s data using regeneratively mode-locked semiconductor laser," *Electron. Lett.*, vol. 39, pp. 453–455, Mar. 2003.

[5] S. Arahira, S. Sasaki, K. Tachibana, and Y. Ogawa, "All-optical 160 Gb/s clock extraction with a mode-locked laser diode module," *IEEE Photon. Technol. Lett.*, vol. 16, pp. 1558–1560, Jun. 2004.

[6] X. Tang, J. C. Cartledge, A. Shen, F. van Dijk, A. Akrout, and G.-H Duan, "Characterization of all-optical clock recovery for 40 Gb/s RZ-OOK and RZ-DPSK data using mode-locked semiconductor lasers," *J. Lightw. Technol.*, vol. 27, pp. 4603–4609, Oct. 2009.

[7] J. Renaudier, B. Lavigne, P. Gallion, and G.-H. Duan, "Study of phase-noise properties and timing jitter of 40-GHz all-optical clock recovery using self-pulsating semiconductor lasers," *J. Ligthw. Technol.*, vol. 24, pp. 3734–3742, Oct. 2006.

[8] M. Costa e Silva, A. Lagrost, L. Bramerie, M. Gay, P. Besnard, M. Joindot, J. C. Simon, A. Shen, and G. H. Duan, "Up to 425 GHz all-optical frequency down-conversion clock recovery based on quantum dash Fabry-Pérot mode-locked," in *Proc. Conf. Opt. Fiber Commun., Collocated. Nat. Fiber Opt. Eng. Conf.*, 2010, pp. 1–3, Paper PDPC4.

[9] F. Lelarge, B. Dagens, J. Renaudier, R. Brenot, A. Accard, F. van Dijk, D. Make, O. Le Gouezigou, J.-G. Provost, F. Poingt, J. Landreau, O. Drisse, E. Derouin, B. Rousseau, F. Pommereau, and G.-H. Duan, "Recent advances on InAs/InP quantum dash based semiconductor lasers and optical amplifiers operating at 1.55 μm," *IEEE J. Sel. Topics Quantum Electron.*, vol. 13, pp. 111–124, Jan./Feb. 2007.

[10] F. Lelarge, F. Pommereau, F. Poingt, L. Le Gouezigou, and O. Le Gouezigou, "Active mode-locking of quantum dot Fabry-Pérot laser diode," in *Proc. IEEE Intl. Semic. Laser Conf.*, 2006, pp. 153–154.

[11] G.-H. Duan, A. Shen, A. Akrout, F. V. Dijk, F. Lelarge, F. Pommereau, O. LeGouezigou, J.-G. Provost, H. Gariah, F. Blache, F. Mallecot, K. Merghem, A. Martinez, and A. Ramdane, "High performance InP-based quantum dash semiconductor mode-locked lasers for optical communications," *Bell Labs Tech. J.*, vol. 14, pp. 63–84, Autumn, 2009.

[12] J. C. Cartledge, X. Tang, M. Yañez, M. Shen, A. Akrout, and G.H. Duan, "All-optical clock recovery using a quantum-dash Fabry–Pérot laser," in *Proc. IEEE Microw. Photon. Conf.*, 2010, pp. 201–204, Paper TH3-1.

[13] R. Maldonado-Basilio, J. Parra-Cetina, S. Latkowski, N. Calabretta, and P. Landais, "Experimental investigation of the optical injection locking dynamics in single section quantum-dash fabry-perot laser diode for packet-based clock recovery applications," *J. Lightw. Technol.*, vol. 31, pp. 860–865, Mar. 2013.

[14] M. Yañez and J. Cartledge, "Single harmonically driven electroabsorption modulator for OTDM demultiplexing," *J. Lightw. Technol.*, vol. 29, pp. 1437–1444, May. 2011.

[15] S. Latkowski, R. Maldonado-Basilio, and P. Landais, "Sub-picosecond pulse generation by 40 GHz passively mode-locked quantum-dash 1-mm-long Fabry-Pérot laser diode," *Opt. Exp.*, vol. 17, pp. 19166–19172, Oct. 2009.

[16] R. Maldonado-Basilio, J. Parra-Cetina, S. Latkowski, and P. Landais, "Timing jitter, optical, and mode-beating linewidths analysis on subpicosecond optical pulses generated by a quantum-dash passively mode-locked semiconductor laser," *Opt. Lett.*, vol. 35, pp. 1184–1186, Apr. 2010.

[17] K. Sato, "100 GHz optical pulse generation using Fabry–Perot laser under continuous wave operation," *Electron. Lett.*, vol. 37, pp. 763–764, Jun. 2001.

[18] R. Maldonado-Basilio, S. Latkowski, S. Philippe, and P. Landais, "40 GHz mode-beating with 8 Hz linewidth and 64 fs timing jitter from a synchronized mode-locked quantum-dash laser diode," *Opt. Lett.*, vol. 36, pp. 3142–3144, Aug. 2011.

[19] J. Parra-Cetina, S. Latkowski, R. Maldonado-Basilio, and P. Landais, "Wavelength tunability of all-optical clock-recovery based on quantum-dash mode-locked laser diode under injection of a 40-Gb/s NRZ data stream," *Photon. Technol. Lett.*, vol. 23, pp. 531–533, May 2011.

[20] J. Lasri, P. Devgan, R. Tang, and P. Kumar, "Self-start optoelectronic oscillator for generating ultra-low-jitter high-rate (10 GHz or higher) optical pulses," *Opt. Exp.*, vol. 11, pp. 1430–1435, Jun. 2003.

[21] K. A. Rauschenbach, K. L. Hall, J. C. Livas, and G. Raybon, "All-optical pulse width and wavelength conversion at 10 Gb/s using a nonlinear optical loop mirror," *Photon. Technol. Lett.*, vol. 6, pp. 1130–1132, Sep. 1994.

[22] S. J. B. Yoo, "Wavelength conversion technologies for WDM network applications," *J. Lightw. Technol.*, vol. 14, pp. 955–966, Jun. 1996.

[23] L. Moller, Y. Su, C. Xie, R. Ryf, X. Liu, X. Wei, and C. R. Doerr, "Enabling 160 Gbit/s transmitter and receiver designs," in *Proc. Opt. Fiber Commun.*, Mar. 2005, vol. 4, Paper OThR3.

[24] B. Lavigne, J. Renaudier, F. Lelarge *et al.*, "Polarization-insensitive low timing jitter and highly optical noise tolerant all-optical 40-GHz clock recovery using a bulk and a quantum-dots-based self-pulsating laser cascade," *J. Lightw. Technol.*, vol. 25, pp. 170–176, Jan. 2007.

[25] J. Renaudier, G. H. Duan, P. Landais, and P. Gallion, "Phase correlation and linewidth reduction of 40 GHz self-pulsation in distributed bragg reflector semiconductor lasers," *IEEE J. Quantum Electron.*, vol. 43, no. 2, pp. 147–156, Feb. 2007.